Int. J. Environ. Sci. Technol. (2014) 11:987–996
DOI 10.1007/s13762-013-0302-4

ORIGINAL PAPER

Raw and calcination-modified coal waste as adsorbents to remove cadmium from simulated mining wastewater

M. Zhang · H. Wang

Received: 6 August 2012 / Revised: 19 March 2013 / Accepted: 23 April 2013 / Published online: 17 May 2013

Abstract The adsorption of cadmium from simulated mining wastewater by coal waste (CW) and calcination-modified coal waste (MCW) was investigated. Effects of pH, initial concentration, particle size of adsorbent, adsorbent dosage and temperature were studied in batch experiments. The adsorption efficiency for cadmium increased with increasing pH, and the optimum pH for cadmium adsorption onto MCW and CW was 6.0 and 6.5, respectively. Kinetic experiments showed that the adsorption equilibrium was reached within 120 min and followed pseudo-second-order model well. The adsorption isotherm data fit Langmuir and Freundlich models, and the adsorption capacity of cadmium on the two adsorbents increased with increasing temperature from 298 to 318 K. MCW had a higher adsorption capacity of cadmium than CW, because calcination treatment can make CW to have more loose structure and higher specific surface area. Thermodynamic parameters, the Gibbs free energy change (ΔG^0), enthalpy change (ΔH^0) and entropy change (ΔS^0), were calculated and the results showed that the adsorption of cadmium on CW and MCW was spontaneous and endothermic. Fourier transform infrared studies indicated silanol and aluminol groups were responsible for cadmium binding. The desorption results indicated that the two adsorbents could be used repeatedly at least three times without significant decrease in the adsorption capacity for cadmium. The results suggested that modified CW could have high potential as low-cost adsorbent for cadmium removal.

Keywords Adsorption · Desorption · Heavy metal · Thermodynamic parameters

Introduction

The release of heavy metals into aquatic ecosystems has caused serious environmental problems because of their toxicity, non-biodegradation and the tendency for accumulation in the food chain (Zhao et al. 2011a, b). Among heavy metals, cadmium is an extremely toxic metal, which is usually found in wastewater from mining, metal plating, smelting, batteries, phosphate fertilizers, pigments, stabilizers, plastics and other industrial process. Excessive exposure to cadmium can cause harmful effects on human health, including itai–itai disease, emphysema, kidney damage and renal damage (Zhu et al. 2007; Munagapati et al. 2010). Therefore, many methods have been developed to remove cadmium from aqueous solution such as chemical precipitation, membrane separation, ion exchange and electrochemistry removal. However, the application of such treatment methods is often restricted because of economic or technical constraints. Adsorption by using low-cost materials is one of the most promising methods to remove heavy metal from wastewater. Many agricultural, industrial and natural waste materials have been used as adsorbents in recent years (Ajmal et al.1998; Gupta and Ali 2004; Villaescusa et al. 2004; Qin et al. 2006; Amuda et al. 2007; Dias et al. 2007; Aydin et al. 2008; Pehlivan et al. 2009; Sthiannopkao and Sreesai 2009; Zvinowanda et al. 2009; Suresh et al. 2012; Zamani et al. 2013), but there are few reports on the application of raw or modified coal waste (CW) in the removal of heavy metal from simulated coal mine wastewater.

There are large amounts of CW generated during coal excavation and subsequent washing processes, which have

M. Zhang (✉) · H. Wang
School of Resources and Environment, University of Jinan, Jinan 250022, China
e-mail: stu_zhangml@ujn.edu.cn

accumulated to nearly 8.0 billon tons at present, and are approaching 380 million tons annually in China. Many CW piles are formed because utilization is usually <30 %. Moreover, a large amount of mining wastewater containing heavy metals can be discharged in the coal mining process, which can result in serious pollution to surrounding soil and water. It will be ideal if the coal mining wastewater containing heavy metals can be treated by physically and/or chemically altered forms of coal waste, and this is just the objective of our present study.

Considering that the chemical activity and adsorption capacity of CW may be improved by calcination treatment, calcination-modified coal waste (MCW) was examined to be one potential low-cost adsorbent in this study. The potential of CW and MCW to remove Cd(II) from coal mining wastewater was evaluated through a series of batch experiments. The effects of pH, initial concentration, adsorbent dosage, particle size of adsorbents and temperature on the adsorption capacity were investigated. Adsorption isotherm models and thermodynamic parameters were also studied to understand the adsorption characteristics. The objective of this study was to establish a fundamental understanding of the adsorption behavior of Cd(II) on CW and MCW, in order to provide a basis for their practical application to mining wastewater treatment. This work was conducted from October to December 2011, in Univeristy of Jinan, China.

Materials and methods

Materials

Coal waste (CW) used in this study was obtained from Zhaolou coal mine in Yuncheng County, Shandong province, China. The adsorbents were ground, dried at 105 °C for 12 h and then stored in a plastic container prior to use. In order to study the effect of calcination modification of CW on the adsorption of Cd(II), one portion of CW sample was calcinated in a furnace at 700 °C for 2 h, cooled in air and then stored in a plastic container as calcination MCW adsorbent in the following experiments (Kakali et al. 2001; Kuang et al. 2012).

All regents used in the present study were all of analytical grade. The stock solution of Cd(II) (10 mmol L^{-1}) was prepared by dissolving $Cd(II)(NO_3)_2 \cdot 4H_2O$ and then diluted to appropriate concentrations. A total of 0.5 mol L^{-1} HNO_3 and NaOH were used for pH adjustment in adsorption experiments, and 0.1 mol L^{-1} HCl was used as the desorption agent in the desorption experiments. 0.05 mol L^{-1} $NaNO_3$ was used as background electrolyte.

Methods

Characteristics of adsorbents

The pH of adsorbent pastes was measured by pH meter (Delta320 METTLER, Germany) in a 1:5 (w/v) solid/water suspension for 24 h to reach equilibrium. The point of zero charge (pH_{PZC}) was determined using the solid addition method (Tripathy and Kanungo 2005). The specific surface area of the adsorbents was measured by the N_2 gas adsorption method with the data BET analysis (Micromeritics, ASAP 2020, USA). Surface morphology of the adsorbents was examined by a scanning electron microscope (SEM, Quanta FEG 250). The SEM was equipped with an energy dispersion spectrometer (EDS, X-Max50), which was used to analyze the chemical constituents of the adsorbents before and after adsorption of Cd(II). Fourier transform infrared (FTIR) spectrometery (RX-1, Perkin-Elmer, USA) was used to determine functional groups of the two adsorbents before and after Cd(II) loading in the wavenumbers range of 400–4,000 cm^{-1}. The FTIR spectra of the samples prepared as KBr pellets were recorded on a Perkin-Elmer Model System 2000. X-ray diffraction (XRD) analysis of CW and MCW was conducted using powder XRD mounts (D/Max-IIIA, Japan) over a 2θ interval of 5–70° with Cu $K\alpha$ radiation.

Batch adsorption experiment

The adsorption experiments were carried out at room temperature (298 K) in 50-mL flasks by mixing 0.3 g adsorbent (60–80 mesh, unless otherwise stated) with 20 mL of 0.2 mmol L^{-1} Cd(II) solution using a shaking thermostat machine at a speed of 200 rpm for 120 min, which was found to be enough to reach adsorption equilibrium. The pH of solution was maintained at 6.0 for MCW and 6.5 for CW by addition of drops of 0.5 mol L^{-1} HNO_3 or NaOH solutions, and solution background electrolyte of 0.05 mol L^{-1} $NaNO_3$ was used (unless otherwise stated).

Kinetic studies were conducted by collecting samples at 5, 10, 20, 30, 60, 120, 180, 240 and 720 min to reveal the contact time for reaching adsorption equilibrium. The effect of solution pH on the adsorption of Cd(II) on the adsorbents was investigated in the range of 2.0–7.0, where Cd(II) precipitation does not occur. The effect of adsorbent dosage was studied by varying the adsorbent dosage from 5 to 50 g L^{-1}. Six different particle sizes of the adsorbents (40–60 mesh, 60–80 mesh, 80-100 mesh, 100-120 mesh, 120-140 mesh, and large than 140 mesh) were selected for the study of effect of particle size on Cd(II) adsorption. For adsorption isotherm study, 0.3 g adsorbent was mixed with 20 mL Cd(II) solutions at various concentrations (0.05–1.5 mmol L^{-1}) and the mixtures were stirred for 120 min in the temperature range of 298–318 K. After adsorption, the adsorbent was filtered by 0.45-um filter paper and the concentration of Cd(II) ions in the solution was analyzed by ICP-OES (Perkin Elme, USA).

The adsorption efficiency of Cd(II) was calculated using Eq. (1) and the adsorption capacity was calculated using Eq. (2).

$$R = \frac{(C_o - C_f)}{C_o} \times 100\,\% \tag{1}$$

$$q = \frac{V(C_o - C_f)}{m} \tag{2}$$

Where R is adsorption efficiency, q is the amount of Cd(II) sorbed per unit mass of the adsorbent (mmol g^{-1}), V is the solution volume (L), m the weight of the adsorbent (g), C_o and C_f initial and final Cd(II) concentration (mmol L^{-1}).

Desorption experiment

0.3 g adsorbents were added into 20 mL of 0.5 mmol L^{-1} Cd(II) under the experimental conditions in the batch adsorption described above. After the adsorption equilibrium, the Cd(II)-loaded adsorbents were placed in another flask and mixed with 50 mL of 0.1 mol L^{-1} HCl solution for 120 min. The mixture was filtered and the desorbed Cd(II) was measured in the filtrate. The adsorbents were washed three times with distilled water to remove remaining acid and reused for next adsorption–desorption cycle. The adsorption–desorption processes were repeated three times. All the above experiments on batch adsorption and desorption were carried out in triplicate and the average results were presented in this study.

Results and discussion

Characteristics of adsorbents

The point of zero charge (pH_{PZC}) of CW and MCW was found to be 5.8 and 5.5, and the paste pH of CW and MCW was 8.3 and 8.1, respectively. The SEM micrographs of the two adsorbents are shown in Fig. 1. It can be seen that the surface morphology of MCW was more porous and loose than that of CW due to calcination treatment. The specific surface area of CW and MCW samples was found to be 3.83 and 9.15 $m^2\ g^{-1}$, respectively, which shows that calcination treatment increased the specific surface area of CW and favoured higher adsorption capacity for Cd(II). The XRD analysis in Fig. 2 shows that the main mineral phases of CW are quartz, kaolinite and illite, while characteristic diffraction peaks for kaolinite disappeared entirely in MCW because kaolinite was converted to amorphous metakaolinite by dehydroxylation when calcinated at around 700 °C (Kakali et al. 2001; Kuang et al. 2012). So calcination modification can make CW to have loose structure and higher activity of chemical reaction.

The FTIR spectra of CW and MCW are shown in Fig. 3. Stretching vibrations of OH− in kaolinite was observed at 3,695.96 and 3,620.19 cm^{-1}, bending vibration of Al–OH at 913.77 cm^{-1}, stretching vibrations of Si–O at 1,010.21 cm^{-1}, 1,034.02 and 1,091.45 cm^{-1}, bending vibrations of Si–O at 471.17 cm^{-1} and stretching vibrations of Si–O–Al^{VI} at 538.79 cm^{-1}. The FTIR spectra described above show the characteristic bands of kaolinite

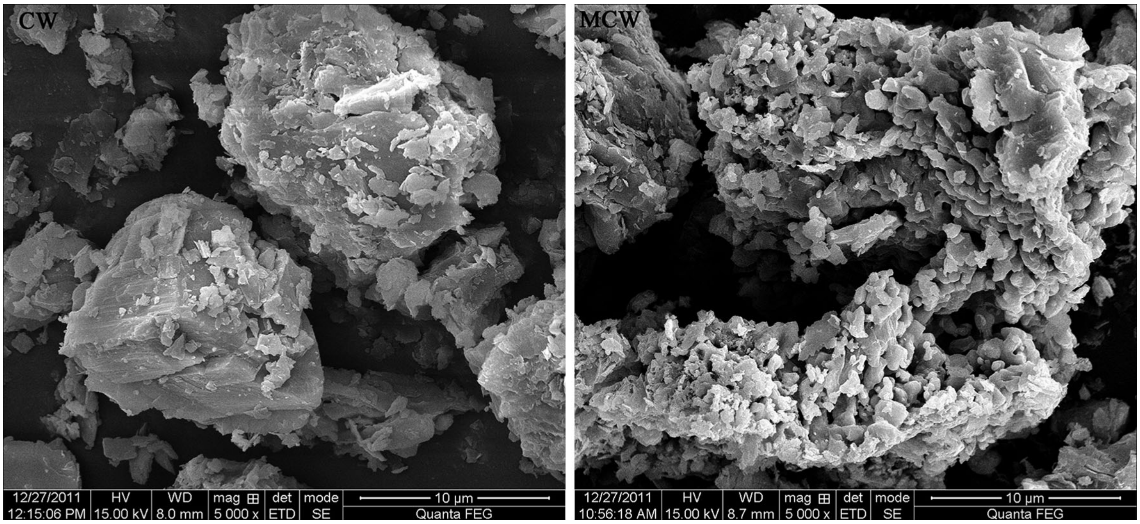

Fig. 1 Scanning electron microscope micrographs of CW and MCW

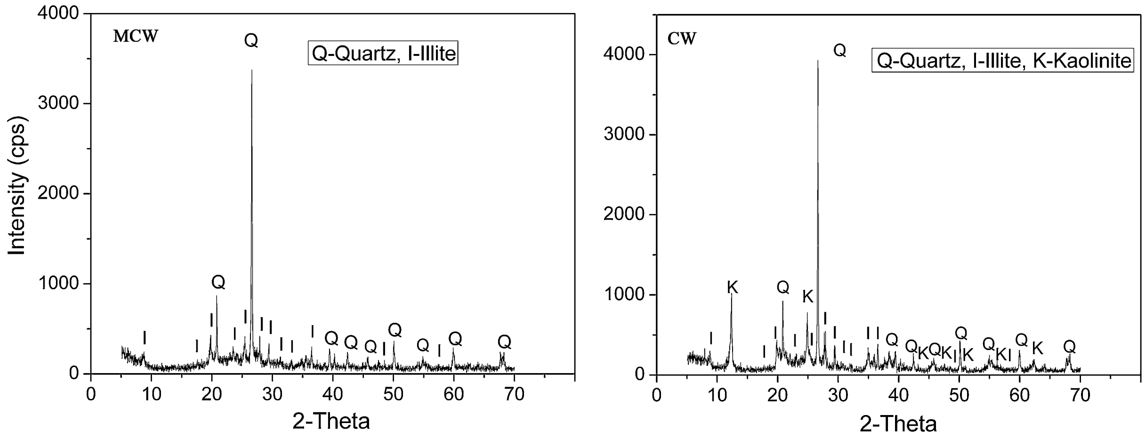

Fig. 2 X-ray diffraction pattern of CW and MCW

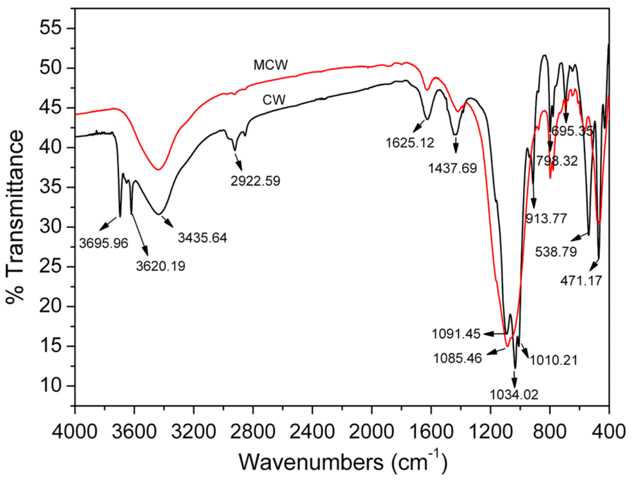

Fig. 3 FTIR spectrum of CW and MCW

(Saikia and Parthasarathy 2010). The bands at 695.35 and 798.32 cm^{-1} could be assigned to symmetry vibration of Si–O–Si. For MCW, Stretching vibrations of OH− at 3,695.96 and 3,620.19 cm^{-1} disappear due to dehydroxylation of kaolinite by calcination treatment at 700 °C, which indicates that crystal structure of kaolinite were decomposed (Kakali et al. 2001). Absence of the detectable characteristic bands of kaolinite, Al–O–H bands at 913.77 cm^{-1}, Si–O bands at 1,010.21, 1,034.02 and 1,091.45 cm^{-1} and Si–O–Al^{VI} at 538.79 cm^{-1}, and the appearance of a new band at 568.30 cm^{-1} (Al–O stretching) can be caused by the change from octahedral coordination of Al^{3+} in kaolinite to tetrahedral coordination in metakaolinite (Kakali et al. 2001). Stretching vibrations of Si–O at 1,085.46 cm^{-1} and bending vibrations of Si–O at 466.76 cm^{-1} appeared in the shape of broadband, which are the characteristic absorption bands of metakaolinite (Kakali et al. 2001; Saikia and Parthasarathy 2010). It is also indicated from FTIR spectra that silanol and aluminol groups are abundant in the adsorbents.

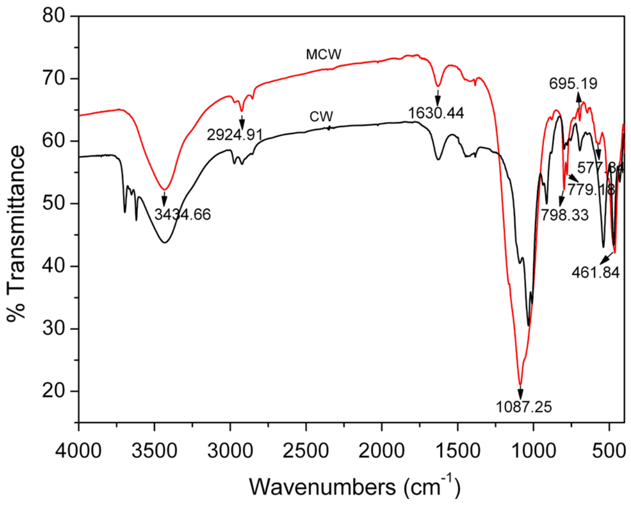

Fig. 4 FTIR spectra for Cd(II)-loaded MCW and CW

The FTIR spectra for Cd(II)-loaded adsorbents was presented in Fig. 4. It shows that the wavenumbers shifted from 568.30 to 577.84 cm^{-1} (Al–O), 466.76 to 461.84 cm^{-1}(Si–O) and 1,085.46 to 1,087.25 cm^{-1}(Si–O), respectively, after Cd(II) adsorption onto MCW. It proved that silanol and aluminol groups were primary contributors involved in the adsorption of Cd(II) onto MCW. While, the functional groups did not shift the peak significantly for CW, only the intensity change of the bands in FTIR spectra after binding with Cd(II) was observed, maybe due to the low adsorption capacity. EDS spectra for MCW and CW after the adsorption of Cd(II) are shown in Fig. 5. EDS spectra (figures not presented) for the raw adsorbents did not show the characteristic signal of Cd(II), while the presence of Cd(II) was observed for the adsorbents after adsorption.

Effect of pH

The adsorption efficiency for Cd(II) increased with increasing pH as expected, and the equilibrium was

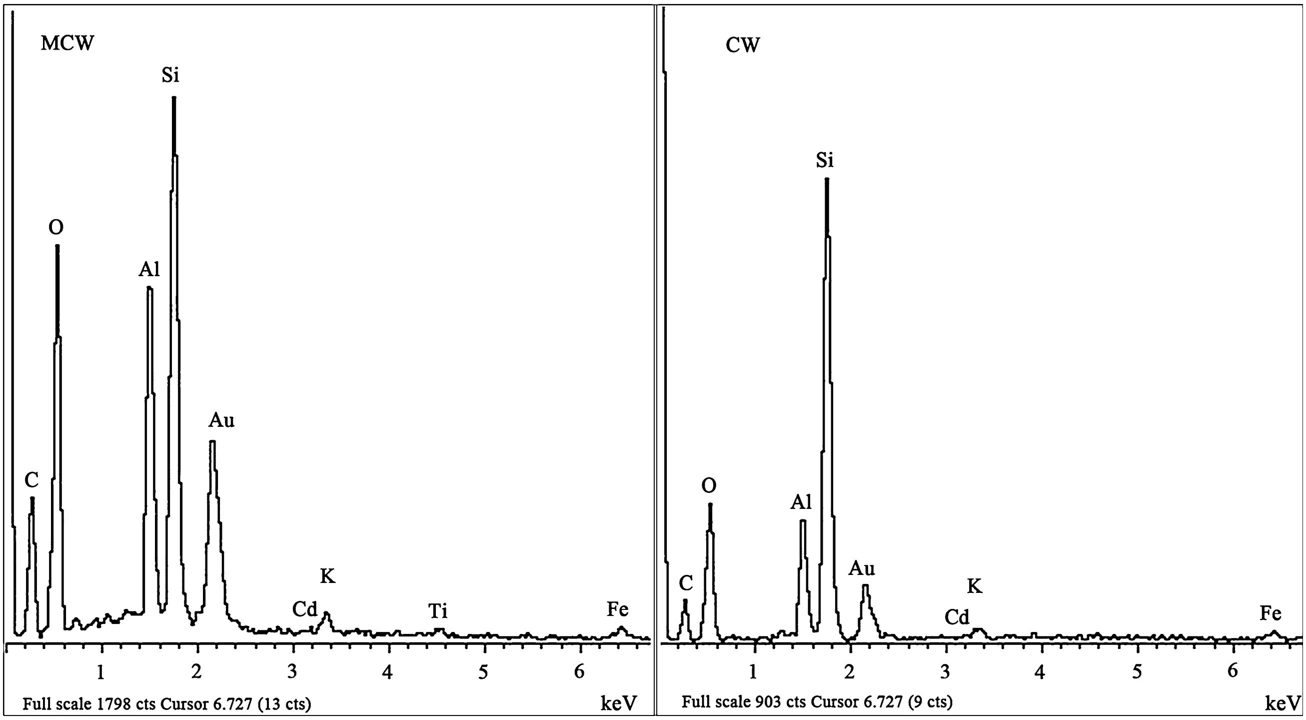

Fig. 5 Energy dispersion spectrometer spectra of MCW and CW after Cd(II) adsorption

achieved above pH_{pzc} (Fig. 6). With pH increasing, the lower number of H^+ and greater number of negatives charges distributed on the adsorbent surface can result in greater Cd(II) adsorption through electrostatic force of attraction. The optimum pH value for adsorption of Cd(II) by the CW and MCW adsorbents was found to be 6.5 and 6.0, respectively, at which the removal efficiency of Cd(II) was observed to be 28.57 and 94.48 %. Therefore, all the following experiments on adsorption of Cd(II) were conducted by maintaining the solution at pH 6.0 for MCW and 6.5 for CW.

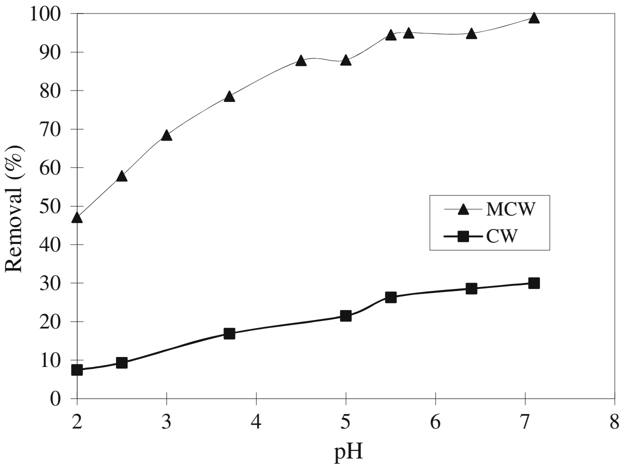

Fig. 6 Effect of pH on adsorption of Cd(II). Experimental conditions: adsorbent dosage 15 g L^{-1}, contact time 120 min, initial concentration 0.2 mmol L^{-1} and T 298 K

The main functional groups of the adsorbents, silanol and aluminol groups, may be responsible for the Cd(II) adsorption on CW and MCW. The silanol groups are negatively charged at low pH range (pH 2–3; near the pH_{PZC} value of silanol), which facilitate the adsorption of Cd(II) in this pH range (Gundogdu et al.2009; Shi et al. 2009). As a result, adsorption can occur even at low pH. Aluminol groups are negatively charged at pH around 6, which further favor the adsorption of Cd(II) on the surface of the adsorbents. The adsorption behavior for Cd(II) can be expressed in Eqs. (3) and (4) (silanol for example):

$$\equiv \mathrm{Si}-\mathrm{OH}+\mathrm{Cd}^{2+} \Leftrightarrow \equiv \mathrm{Si}-\mathrm{OCd}^{+}+\mathrm{H}^{+} \tag{3}$$

$$\equiv \mathrm{Si}-\mathrm{O}^{-}+\mathrm{Cd}^{2+} \Leftrightarrow \equiv \mathrm{Si}-\mathrm{OCd}^{+} \tag{4}$$

Effect of the initial concentration

The effect of initial Cd(II) concentration on the adsorption efficiency was investigated in the range of 0.05–1.5 mmol L^{-1} at 298, 308 and 318 K. The results show that the adsorption efficiency decreased with increasing initial Cd(II) concentration. The lower adsorption efficiency at higher concentration resulted from an increasing ratio of initial number of moles of Cd(II) to the available adsorption sites. The available adsorption site was fixed per mass of adsorbent dose. Accordingly, it resulted in a decrease in the removal efficiency of metal

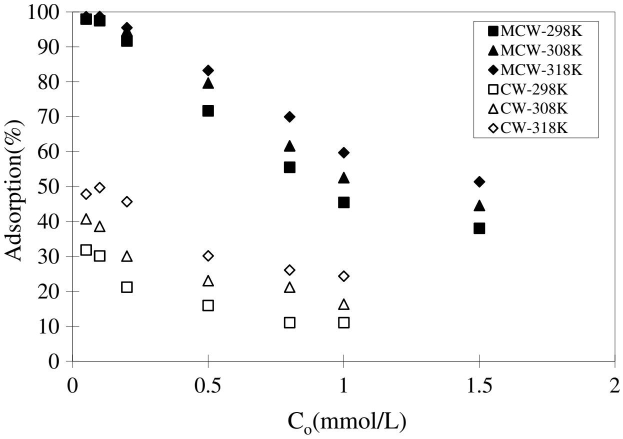

Fig. 7 Effect of initial ion concentration on adsorption of Cd(II). Experimental conditions: pH 6.0 for MCW and 6.5 for CW, adsorbent dosage 15 g L^{-1}, contact time 120 min and T 298 K

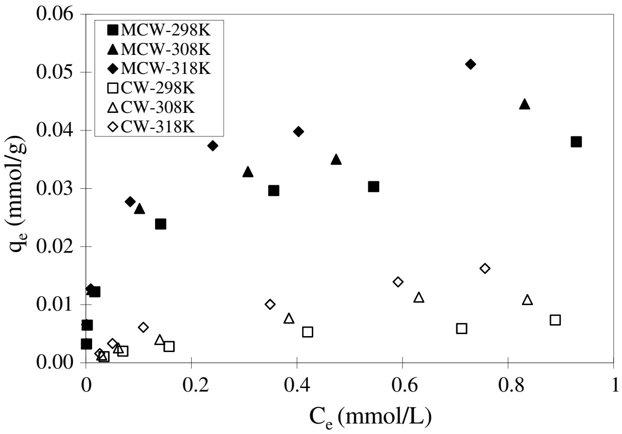

Fig. 8 The adsorption isotherms for adsorption of Cd(II) on MCW and CW at 298, 308 and 318 K. Experimental conditions: pH 6.0 for MCW and 6.5 for CW, adsorbent dosage 15 g L^{-1} and contact time 120 min

ion, with increase in initial metal ion concentration (saturation of the adsorbent). It is also observed that the adsorption efficiencies of Cd(II) onto CW and MCW increased with temperature increasing from 298 to 318 K (Fig. 7). For example, at the initial concentration of 0.5 mmol L^{-1}, the adsorption efficiencies of Cd(II) onto CW and MCW increased from 71.68 to 83.24 % and from 23.09 to 30.20 %, respectively, with temperature increasing from 298 to 318 K.

Effect of adsorbent dosage

It is observed that with the adsorbent dosage increasing from 5 to 50 g L^{-1}, the adsorption efficiency of Cd(II) increased, while the adsorption capacity decreased. Because of the higher adsorbent dosage in the solution, more available adsorption sites are available and more Cd(II) were adsorbed. The decrease in adsorption capacity of Cd(II) with the adsorbent dosage increasing is due to the existence of unsaturated adsorption sites (Ho and Mckay 1998; Manohar et al. 2002). It is also observed that the adsorption efficiency of Cd(II) was not increased significantly when the adsorbent dosage is higher than 15 g L^{-1}, which was chosen as the optimum adsorbent dosage. The active adsorption sites on the adsorbent surface are then occupied and further increase in the adsorbent dosage cannot bring higher adsorption efficiency.

Effect of particle size

The results show that adsorption efficiency of Cd(II) increased from 86.86 to 95.54 % and from 18.34 to 37.61 % for MCW and CW, as the particle size of the adsorbents decreased from 40 to 60 mesh to 80 to 100 mesh. With the particle size decreasing, the surface area of adsorbent will increase and more adsorption sites are available for Cd(II) to be adsorbed. Hence, adsorption efficiency will be enhanced. However, when particle size decreased to a sufficient extent (smaller than 100 mesh), the adsorption efficiency increased <2 %, and it had no significant influence on Cd(II) adsorption.

Adsorption isotherms

The Langmuir and Freundlich models were used to simulate adsorption isotherms. The linear forms of the Langmuir and Freundlich isotherms are presented by Eqs. (5) and (6).

$$\frac{C_e}{q_e} = \frac{1}{bq_{\max}} + \frac{C_e}{q_{\max}} \tag{5}$$

$$\log q_e = \log K_F + \frac{1}{n} \log C_e \tag{6}$$

Where q_e is the amount adsorbed per mass of adsorbent at equilibrium (mmol g^{-1}), C_e is the concentration of adsorbate at equilibrium (mmol L^{-1}), $q_{\max}$ is the maximum adsorption capacity (mmol g^{-1}) and b (L mol^{-1}) is the adsorption equilibrium constant related to adsorption energy. K_F (mmol g^{-1}) and $1/n$ (unitless) are the Freundlich constants related to adsorption capacity and intensity, respectively.

The essential feature of the Langmuir model can be described by using a separation factor (R_L), which is defined by Eq. (7).

$$R_L = \frac{1}{1 + bC_o} \tag{7}$$

Where R_L values indicate the type of isotherm as being favorable adsorption ($0 < R_L < 1$), unfavorable adsorption ($R_L > 1$), linear adsorption ($R_L = 1$) or irreversible adsorption ($R_L = 0$).

Table 1 Parameters of the Langmuir and Freundlich isotherm models of Cd(II) adsorption at 298, 308 and 318 K

Adsorbent	*T* (K)	Langmuir	Freundlich					
		$q_{\max}$ (mmol g^{-1})	b (L mol^{-1})	R^2	R_L	K_F (mmol g^{-1})	*n*	R^2
MCW	298	0.037	21.016	0.98	0.03–0.49	0.041	2.991	0.97
	308	0.044	23.051	0.97	0.03–0.46	0.051	2.908	0.96
	318	0.051	23.556	0.97	0.03–0.46	0.061	2.757	0.98
CW	298	0.009	3.46	0.97	0.22–0.85	0.008	1.783	0.97
	308	0.016	2.842	0.95	0.26–0.88	0.014	1.578	0.98
	318	0.022	3.112	0.97	0.24–0.87	0.02	1.553	0.96

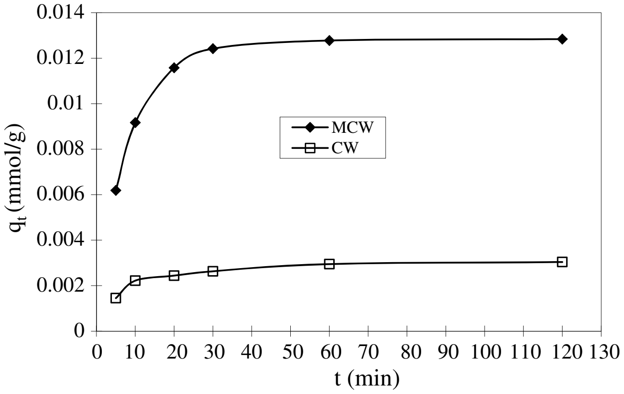

Fig. 9 The adsorption kinetic for adsorption of Cd(II). Experimental conditions: pH 6.0 for MCW and 6.5 for CW, adsorbent dosage 15 g/l, contact time 120 min, initial concentration 0.2 mmol/L and T 298 K

The plots of the adsorption isotherm of Cd(II) on CW and MCW at different temperatures (298, 308 and 318 K) are shown in Fig. 8. The parameters for Langmuir and Freundlich isotherm models are listed in Table 1. It shows that the Langmuir and Freundlich models fit well for the adsorption of Cd(II) on the two adsorbents with the high values of R^2 (0.95–0.98). The maximum adsorption capacity ($q_{\max}$) increased from 0.037 to 0.051 mmol g^{-1} (MCW) and from 0.009 to 0.022 mmol g^{-1} (CW) with temperature increasing from 298 to 318 K. This suggested that the adsorption of Cd(II) onto the two adsorbents was endothermic in nature, which is proved by adsorption thermodynamic parameters described below. It was also obvious that the $q_{\max}$ of Cd(II) on MCW was larger than that of CW, as calcination treatment increased the adsorption capacity. However, the adsorption capacities of CW and MCW are lower, compared with some other adsorbents in literature (Ajmal et al. 2003; Naiya et al. 2009).

The Langmuir constant, *b*, related to adsorption energy indicates the strength and affinity of the adsorbents for the solute. For the adsorption of Cd(II) on MCW, it was about seven times larger than for CW and it increased with increasing temperature, while for CW adsorbent, the Langmuir constant, *b*, decreased with increasing temperature. This indicated that Cd(II) had higher affinity toward the surface of MCW than CW and the adsorption process may be more stable on MCW than on CW. All the values of R_L were in the range of 0.03–0.49 for MCW and 0.22–0.87 for CW for the initial Cd(II) concentration range of 0.05 to 1.5 mmol L^{-1}, indicating favorable adsorption of Cd(II) onto the two adsorbents.

As expected, the values of Freundlich constant K_F for the adsorption on MCW were greater than that of adsorption on CW, and the value of K_F all increased with temperature increasing from 298 to 318 K. The values of *n* between 1 and 10 (i.e., $1/n < 1$) represent a favorable adsorption (Naiya et al. 2009).

Kinetics

Kinetic analysis was conducted by pseudo-first-order and pseudo-second-order models. The linear forms of the kinetic models are given in Eqs. (8) and (9)

$$\log(q_e - q_t) = \log q_e - \frac{k_1 t}{2.303} \tag{8}$$

$$\frac{t}{q_t} = \frac{1}{k_2 q_e^2} + \frac{1}{q_e} t \tag{9}$$

Where q_t is the amount of Cd(II) adsorbed by MCW or CW at time *t* (mmol g^{-1}), and k_1(min^{-1}), k_2(g mmol min^{-1}) are the rate constants of the pseudo-first-order model and pseudo-second-order model, respectively; *t* is the adsorption time (min).

The adsorption of Cd(II) on the two adsorbents showed typical biphasic kinetics with rapid adsorption in the first 10 min, and then, the adsorption capacity slowly reached equilibrium. This is because initially abundant active sites are available for adsorption and Cd(II) concentration gradient is high. Afterward, few surface active sites become available and difficult to be occupied due to repulsive forces between the solute molecules of the solid and bulk phase; therefore, very slow increase in the Cd(II) adsorption is observed. Adsorption equilibrium was achieved within 120 min for Cd(II) adsorption onto the two adsorbents. Thus, 120 min of contact time was considered as the optimum time in each adsorption experiment.

Table 2 Theoretically determined parameters of pseudo–first order and pseudo–second order

Adsorbent	Experimental q_e (mmol g^{-1})	Pseudo–first order			Pseudo–second order		
		q_e (mmol g^{-1})	k_1 (min^{-1})	R^2	q_e (mmol g^{-1})	k_2 (g mmol·min^{-1})	R^2
MCW	0.012	0.004	0.127	0.93	0.013	19.304	0.99
CW	0.003	0.001	0.062	0.92	0.003	57.184	0.99

Table 3 Thermodynamic parameters of Cd(II) adsorption on MCW and CW at 298, 313 and 318 K

Adsorbent	Temperature (K)	ΔG^0 (kJ mol^{-1})	ΔH^o (kJ mol^{-1})	ΔS^o (J mol^{-1} K^{-1})
MCW	298	−17.24	19.75	124.12
	308	−18.65		
	318	−19.73		
CW	298	−8.3	32.23	135.83
	308	−9.58		
	318	−11.03		

The adsorption kinetic for adsorption of Cd(II) is shown in Fig. 9. The kinetic parameters of Cd(II) adsorption on CW and MCW are presented in Table 2. As shown, the theoretical q_e values calculated from pseudo–first order had significant difference compared to experimental values, and the correlation coefficients (R^2) were very low, while the pseudo-second-order model described the experimental data well, evidenced by correlation coefficients (R^2) close to 1 and the theoretical q_e values of Cd(II) almost equal to the experimental q_e values. This indicates that the rate-limiting step may be the chemical adsorption (Ding et al. 2006).

Thermodynamic parameters

In the thermodynamic study, the thermodynamic parameters, that is, the Gibbs free energy (ΔG^0), enthalpy (ΔH^0) and entropy (ΔS^0) changes, were determined by using the following equations (Yang et al. 2011; Zhao et al. 2011a, b):

$$\Delta G^o = -RT \ln K^o \qquad (10)$$

where R is the ideal gas constant (8.314 J mol·K^{-1}); T is the Kelvin temperature; K^o, the adsorption equilibrium constant, is obtained by plotting ln K_d versus C_e and extrapolating C_e to zero. The intercept value is that of ln K^o. The distribution adsorption coefficient, K_d, can be determined from Eq. (11) (Zhao et al. 2011a, b):

$$K_d = \frac{C_o - C_e}{C_e} \cdot \frac{V}{m} \qquad (11)$$

The enthalpy change (ΔH^0) and entropy change (ΔS^0) can be calculated from the slope and intercept of the plot of ln K^o versus 1/T by Eq. (12).

$$\ln K^0 = \frac{\Delta S^0}{R} - \frac{\Delta H^0}{RT} \qquad (12)$$

The thermodynamic parameters were calculated from the adsorption isotherms of Cd(II) on CW and MCW at different temperatures. According to Eq(12), the slope and intercept of the plot of ln K^o versus 1/T were calculated, respectively.

Thermodynamic parameters of Cd(II) adsorption on CW and MCW calculated from Eqs. (10)–(12) were presented in Table 3. The negative Gibbs free energy change (ΔG^0) indicates that the adsorption process is spontaneous. The values of ΔG^0 decreased with the temperature increasing from 298 to 318 K, which indicates the endothermic adsorptions of Cd(II) onto CW and MCW were enhanced with increasing temperature. The enthalpy of the adsorption, ΔH^0, is a indication of the energy barrier that must be overcome during the adsorption process by reacting molecules (Unuabonah et al. 2008). The positive ΔH^0 suggests that the adsorption reaction onto the two adsorbents are endothermic in nature, which shows that increasing temperature will promote the adsorption of Cd(II) onto the adsorbents. This is an indication of chemical reaction or bonding process being involved in Cd(II) adsorption process; thus, the adsorption processes may belong to chemical sorption. The value of ΔS^0 can determine whether the adsorption process is associative or dissociative mechanism. Generally, entropy change $\Delta S^0 > -10^{-2}$ kJ $Kmol^{-1}$ indicates dissociative mechanism (Scheckel and Sparks 2001; Shi et al. 2009; Zhao et al. 2011a, b). The values of ΔS^0 of Cd(II) adsorption on the two adsorbents were all positive, which indicated that dissociative mechanism could be involved in the adsorption processes (Shi et al. 2009; Zhao et al. 2011a, b).

Desorption

The desorption results are shown in Table 4, which showed that the two adsorbents could be used repeatedly at least three times without significant decrease in the adsorption capacity for Cd(II). It is also observed that Cd(II) desorption for MCW was generally smaller than that of CW, which suggests that the MCW bind Cd(II) ion more strongly than CW. This strongly correlated with the earlier suggestion from the binding energy constant (*b*).

Table 4 Adsorption and desorption amount of Cd(II) by CW and MCW in adsorption–desorption cycles

Adsorbent	Cycle no.	Amount before adsorption (mmol L^{-1})	Amount after adsorption (mmol L^{-1})	Adsorption (%)	Amount desorbed with 0.1 mol L^{-1} HCl (mmol L^{-1})	Recovery (%)
MCW	1	0.5	0.132	73.6	0.339	92.12
	2	0.5	0.141	71.8	0.321	89.42
	3	0.5	0.136	72.8	0.316	86.81
CW	1	0.5	0.416	16.8	0.081	96.43
	2	0.5	0.422	15.6	0.072	92.31
	3	0.5	0.435	13	0.059	90.77

Conclusion

Calcination treatment can impart loose structure and higher specific surface area to coal waste, enabling calcination-treated CW to have a higher adsorption capacity for Cd(II). The adsorption of Cd(II) on the adsorbents increased with increasing temperature from 298 to 318 K. The adsorption efficiency for Cd(II) increased with increasing pH, and the optimum pH value for adsorption of Cd(II) by the CW and MCW adsorbents was found to be 6.5 and 6.0, respectively. It is observed that the adsorption efficiency of Cd(II) was not increased significantly when adsorbent dosage was higher than 15 g L^{-1}, which was considered as an optimum adsorbent dosage level at the specified conditions. The equilibrium of the adsorption can be reached within 120 min, and the process can be simulated by pseudo-second-order model. Thermodynamic analysis showed the adsorption processes were endothermic and spontaneous processes, and they may be chemical in nature with positive ΔH^0; the positive ΔS^0 suggests that dissociative processes were involved in the adsorption of Cd(II). The desorption results indicated that the two adsorbents could be used repeatedly (at least three times) without significant decrease in the adsorption capacity for Cd(II). The FTIR studies indicated that silanol and aluminol were primary functional groups responsible for metal binding.

Acknowledgments This work was supported by Shandong Provincial Natural Science Foundation, China (ZR2010DQ005, ZR2010DL005), the Natural Science Foundation of China (41172222) and Doctoral Foundation of University Jinan (XBS1036).

References

Ajmal M, Khan AH, Ahmad S, Ahmad A (1998) Role of sawdust in the removal of copper (II) from industrial wastes. Water Res 22:3085–3091

Ajmal M, Rao R, Anwar JA, Ahmad R (2003) Adsorption studies on rice husk: removaland recovery of Cd (II) from wastewater. Bioresour Technol 86:147–149

Amuda OS, Giwa AA, Bello IA (2007) Removal of heavy metal from industrial wastewater using modified activated coconut shell carbon. Biochem Eng J 36:174–181

Aydin H, Bulut Y, Yerlikaya C (2008) Removal of copper (II) from aqueous solution by adsorption onto low-cost adsorbents. J Environ Manage 87:37–45

Dias JM, Alvim-Ferraz MCM, Almeida MF, Rivera-Utrilla J, Sanchez-Polo M (2007) Waste materials for activated carbon preparation and its use in aqueous phase treatment: a review. J Environ Manage 85:833–846

Ding P, Huang K, Li G, Liu Y, Zeng W (2006) Kinetics of adsorption of Zn(II) ion on chitosan derivatives. Int J Biol Macromol 39:222–227

Gundogdu A, Ozdes D, Duran C, Bulut VN, Soylak M (2009) Biosorption of Pb(II) ions from aqueous solution by pine bark (*Pinus brutia Ten.*). Chem Eng J 153:62–69

Gupta VK, Ali I (2004) Removal of lead and chromium from wastewater using bagasse fly ash-a sugar industry waste. J Colloid Interface Sci 271:321–328

Ho YS, McKay G (1998) Kinetic models for the sorption of dye from aqueous solution by wood. J Environ Sci Health Part B Process Saf Environ Prot 76:183–191

Kakali G, Perraki T, Tsivilis S, Badogiannis E (2001) Thermal treatment of kaolin: the effect of mineralogy on the pozzolanic activity. Appl Clay Sci 20:73–80

Kuang J, Qiu T, Shi F (2012) Effect of heat treatment on structure transformation and activities of kaolinite. Chin J Nonferrous Metals 22:258–264

Manohar DM, Krishnan KA, Anirudhan TS (2002) Removal of mercury(II) from aqueous solutions and chlor-alkali industry wastewater using 2-mercaptobenzimidazole-clay. Water Res 36:1609–1619

Munagapati VS, Yarramuthi V, Nadavala SK, Alla SR, Abburi K (2010) Biosorption of Cu(II), Cd(II) and Pb(II) by Acacia leucocephala bark powder: kinetics, equilibrium and thermodynamics. Chem Eng J 157:357–365

Naiya TK, Bhattacharya AK, Mandal S, Das SK (2009) The sorption of lead(II) ions on rice husk ash. J Hazar Mater 163:1254–1264

Pehlivan E, Altun T, Cetin S, Bhanger MI (2009) Lead sorption by waste biomass of hazelnut and almond shell. J Hazard Mater 167:1203–1208

Qin F, Wen B, Shan XQ, Xie YN, Liu T, Zhang SZ, Khan SU (2006) Mechanisms of competitive adsorption of Pb, Cu, and Cd on peat. Environ Pollut 144:669–680

Saikia BJ, Parthasarathy G (2010) Fourier Transform Infrared Spectroscopic Characterization of Kaolinite from Assam and Meghalaya, Northeastern India. J Mod Phys 1:206–210

Scheckel KG, Sparks DL (2001) Temperature effects on nickel sorption kinetics at the minera-water interface. Soil Sci Soc Am J 65:719–728

Shi T, Jia S, Chen Y, Wen Y, Dua C, Guo H, Wang Z (2009) Adsorption of Pb(II), Cr(III), Cu(II), Cd(II) and Ni(II) onto a vanadium mine tailing from aqueous solution. J Hazard Mater 169:838–846

Sthiannopkao S, Sreesai S (2009) Utilization of pulp and paper industrial wastes to remove heavy metals from metal finishing wastewater. J Environ Manage 90:3283–3289

Suresh S, Kamsonlian S, Majumder CB, Chand S, Ramanaiah V, Kumar A (2012) Biosorptive behaviour of mango leaf powder and rice husk for arsenic(III) from aqueous solutions. Int J Environ Sci Technol 9:565–578

Tripathy SS, Kanungo SB (2005) Adsorption of Co^{2+}, Ni^{2+}, Cu^{2+} and Zn^{2+} from 0.5 M NaCl and major ion sea water on a mixture of δ-MnO2 and amorphous FeOOH. J Colloid Interf Sci 284:30–38

Unuabonah EI, Adebowale KO, Olu-owolabi BI, Yang LZ, Kong LX (2008) Adsorption of Pb(II) and Cd (II) from aqueous solutions onto sodium tetraborate-modified Kaolinite clay: equilibrium and thermodynamic studies. Hydrometallurgy 93:1–9

Villaescusa I, Fiol N, Martinez M, Miralles N, Pocj J, Serarols J (2004) Removal of copper and nickel ions from aqueous solutions by grape stalks wastes. Water Res 38:992–1002

Yang X, Yang SB, Yang ST, Hu J, Tan XL, Wang XK (2011) Effect of pH, ionic strength and temperature on sorption of Pb(II) on NKF-6 zeolite studied by batch technique. Chem Eng J 168:86–93

Zamani AA, Shokri R, Yaftian MR, Parizanganeh AH (2013) Adsorption of lead, zinc and cadmium ions from contaminated water onto Peganum harmala seeds as biosorbent. Int J Environ Sci Technol 10:93–102

Zhao X, Zhang G, Jia Q, Zhao C, Zhou W, Li W (2011a) Adsorption of Cu(II), Pb(II), Co(II), Ni(II), and Cd(II) from aqueous solution by poly (aryl ether ketone) containing pendant carboxyl groups (PEK-L): equilibrium, kinetics, and thermodynamics. Chem Eng J 171:152–158

Zhao G, Li J, Wang X (2011b) Kinetic and thermodynamic study of 1-naphthol adsorption from aqueous solution to sulfonated graphene nano sheets. Chem Eng J 173:185–190

Zhu C, Luan Z, Wang Y, Shan X (2007) Removal of cadmium from aqueous solutions by adsorption on granular red mud (GRM). Sep Purif Technol 57:161–169

Zvinowanda CM, Okonkwo JO, Shabalala PN, Agyei NM (2009) A novel adsorbent for heavy metal remediation in aqueous environments. Int J Environ Sci Technol 6:425–434